

An x-ray resonant diffraction study of multiferroic DyMn₂O₅

R. A. Ewings,^{1,*} A. T. Boothroyd,¹ D. F. McMorrow,² D. Mannix,³ H. C. Walker,² and B. M. R. Wanklyn¹

¹ *Department of Physics, University of Oxford, Oxford, OX1 3PU, United Kingdom*

² *London Centre for Nanotechnology and Department of Physics and Astronomy,
University College London, London, WC1E 6BT, United Kingdom*

³ *XMaS CRG Beam line, European Synchrotron Radiation Facility, F-38043 Grenoble, France*

(Dated: February 2, 2008)

X-ray resonant scattering has been used to measure the magnetic order of the Dy ions below 40 K in multiferroic DyMn₂O₅. The magnetic order has a complex behaviour. There are several different ordering wavevectors, both incommensurate and commensurate, as the temperature is varied. In addition a non-magnetic signal at twice the wavevector of one of the commensurate signals is observed, the maximum intensity of which occurs at the same temperature as a local maximum in the ferroelectric polarisation. Some of the results, which bear resemblance to the behaviour of other members of the RMn₂O₅ family of multiferroic materials, may be explained by a theory based on so-called acentric spin-density waves.

PACS numbers: 61.10.Nz, 75.47.Lx, 75.25.+z

I. INTRODUCTION

In recent years there has been an upsurge in research into materials which display coupling between ferromagnetic and ferroelectric order parameters. Such materials, which are members of the class known as multiferroics, have been known to science for some time^{1,2,3,4,5,6,7,8}, however recent discoveries of compounds in which the magneto-electric coupling is strong have sparked a renaissance. Of particular interest are the RMnO₃ and RMn₂O₅ (R = rare earth) materials. Indeed, the current revival of the multiferroic field was stimulated by measurements on TbMnO₃^{9,10}, which shows an unprecedentedly strong magneto-electric coupling.

A common feature of these manganese oxide based compounds is a complex magnetic phase diagram, including magnetic order that is in turn antiferromagnetic, incommensurate and/or commensurate in wavevector^{9,10,11}. Another common feature is the possibility to control ferroelectric (FE) polarisation by the application of a moderate magnetic field. This control can take the form of enhancing, creating, or switching the direction of the polarisation. Several theories, based on symmetry considerations, have been proposed to explain such phenomena^{12,13}.

The bulk properties of the RMn₂O₅ (R = Tb, Ho, Er, Dy, ...) compounds have been studied in some detail and have many similar features^{14,15,16,17,18}. In zero applied magnetic field there exists a finite FE polarisation along the b -axis in the approximate temperature range $20 \leq T \leq 35$ K, which increases rapidly at the lower end of the temperature range and decreases more gradually at the upper end. Such behaviour is present for all RMn₂O₅ compounds, however the magnitude of the polarisation is largest in DyMn₂O₅, and appears to be significantly weaker if R is a non-magnetic ion such as Y¹⁸. It would seem, therefore, that the presence of a magnetic rare-earth enhances the FE polarisation.

The temperature dependence of the FE polarisation of

DyMn₂O₅ is somewhat complicated¹⁷. Below about 7K the polarisation is negligibly small, however for $7 \leq T \leq 12$ K the polarisation is small but no longer negligible. Between 12K and 15K there is a sharp rise in polarisation, with a maximum just above 15K. The polarisation then steadily falls with increasing temperature up to about 22K. Above this temperature the polarisation rises again, reaching a local maximum (which is slightly lower than the polarisation at 15K) at about 25K. Further increase of temperature results in a steady reduction of polarisation, until it becomes zero at about 39K. Higashiyama *et al* have labelled three different ferroelectric phases as follows: FE3 for $7 \leq T \leq 14$ K, FE2 for $14 < T \leq 27$ K, and FE1 for $27 < T \leq 39$ K. The upper temperature limit of the polarisation is independent of applied magnetic field, as is the existence of a sharp spike in the dielectric permittivity. If a magnetic field is applied along a particular crystallographic axis (which axis is material dependent, it seems) then ferroelectric effects occur at lower temperatures, including increased polarisation, a switching of the direction of polarisation and increases in the dielectric permittivity.

As well as the ferroelectric phase, other common features among RMn₂O₅ compounds are the existence of a magnetic transition from an ordered to a disordered state at $T_N \sim 40$ K, with a transition into a ferroelectric state just below T_N . At low temperatures, typically $T < 10$ K, the magnetic rare earth ions are observed to order antiferromagnetically. The precise details of these changes are different, depending on the choice of R . This may depend on the magnetic easy axis of the material, which is the a -axis for R = Tb, the b -axis for R = Dy and Ho, and the c -axis for R = Er and Tm. All of these transitions are accompanied by distinct anomalies in the specific heat.

DyMn₂O₅ crystallises in the orthorhombic space group $Pbam$ with the lattice parameters $a = 7.294$ Å, $b = 8.555$ Å and $c = 5.688$ Å. The structure is such that interspersed between sheets of Dy³⁺ ions there are, in order along the c -axis, a Mn⁴⁺O₆ octahedron, a Mn³⁺O₅

bipyramid, followed by another Mn^{4+}O_6 octahedron¹⁹.

There have been several neutron scattering experiments conducted on DyMn_2O_5 ^{19,20,21}. These experiments have had some success in elucidating the crystallographic and magnetic structure of this material. It appears that there are three distinct magnetic phases present at various temperatures below T_N . Below $T \approx 8$ K the Dy ions are modulated antiferromagnetically (AFM) along the a -axis, with wavevector $\mathbf{q}_{AFM}^{Dy} = (0.5, 0, 0)$, with their moments pointing along the b -axis. From base temperature up to T_N the Mn^{3+} and Mn^{4+} ions undergo several magnetic transitions between an incommensurate magnetic (ICM) phase and a commensurate magnetic (CM) phase. The propagation vectors of these phases will be denoted hereafter by \mathbf{q}_{ICM} and \mathbf{q}_{CM} respectively, where $\mathbf{q}_{ICM} = (0.5 \pm \delta, 0, 0.25 \pm \epsilon)$ and $\mathbf{q}_{CM} = (0.5, 0, 0.25)$. The existence of these phases has been shown in all the neutron scattering measurements, but the precise details of ordering wavevectors and temperatures are not consistent between studies.

Wilkinson *et al.*²⁰ measured the magnetic structure at 4.2 K and found, coexisting with the AFM order of the Dy ions, an ICM structure with $\delta = 0$ but $\epsilon \neq 0$. The value of ϵ was found to vary slightly in the range $0 \leq \epsilon \leq 0.002$ for the three temperatures measured (4.2 K, 18 K and 44 K). This incommensurate order was attributed to the ordering of both sets of Mn ions. More recently, neutron powder diffraction measurements by Blake *et al.*¹⁹ were able to resolve a magnetic structure with $\delta = 0.01$ and $\epsilon = 0$ below 32 K, which they did not observe to change on cooling until $T \leq 8$ K, whereupon it became much weaker and an AFM phase the same as that seen by Wilkinson *et al.* was found.

Subsequently, single crystal neutron diffraction measurements were made by Ratcliff *et al.*²¹ over a temperature range $2 \text{ K} \leq T \leq 45 \text{ K}$. Like the other measurements they found an AFM phase below 8 K, but at higher temperatures they found a more complex behaviour. Two different ICM phases were found for $8 \text{ K} \leq T \leq 18 \text{ K}$ characterised by the wavevector $\mathbf{q}_{ICM} = (0.5, 0, 0.25 + \epsilon_{1,2})$, where $\epsilon_{1,2}$ are two different incommensurabilities which vary in size between 0 and 0.02 and have opposite sign. For $18 \text{ K} \leq T \leq 33 \text{ K}$ one of the ICM peaks becomes CM whilst the other's intensity gradually decreases with increasing temperature. For $T > 33 \text{ K}$ there exists only the CM phase, and on warming this disappears by $\sim 40 \text{ K}$.

Up to now there have been no x-ray resonant scattering (XRS) studies of DyMn_2O_5 , although there have been two XRS studies of the related compound TbMn_2O_5 ^{22,23}, both of which have concerned themselves with the ordering of the Mn sublattice by tuning the incident x-ray energy to one of the Mn edges. For $10 \leq T \leq 41 \text{ K}$ a pair of ICM peaks at $(0.5 \pm \delta, 0, 0.25 + \epsilon)$ are observed, where δ decreases from about 0.012 at 10 K to 0.003 at 25 K, where it remains constant until 32 K above which it increases to about 0.012 at 41 K. The c -axis incommensurability ϵ gradually decreases from 0.06 at 10 K to 0.03 at 41 K. The intensity of the ICM peaks decreases steadily with

increasing temperature. Above about 21 K a CM peak at $(0.5, 0, 0.25)$ appears, the intensity of which increases with increasing temperature up to about 30 K, and then decreases on further warming to 41 K. It is also noted that the $(3, 0, 0)$ Bragg peak, which is forbidden in the $P6_{3mm}$ space group that characterises the crystal structure of TbMn_2O_5 , is observed to scale exactly as the FE polarisation squared. The $(3, 0, 0)$ Bragg peak would be allowed if the space group became non-centrosymmetric, and lack of a centre of inversion is required in all of the proposed explanations for the occurrence of FE polarisation in magnetically ordered materials.

There were several motivations for this XRS study of DyMn_2O_5 . Firstly, XRS offers the possibility of probing the magnetic order on the Dy and Mn sites separately by using the resonant enhancement in the scattering when the x-ray energy is tuned to an atomic absorption edge. Neutron diffraction, by contrast, is sensitive only to the size of the overall magnetic moment and not to the atomic species to which it is attached. Secondly, XRS offers a high wavevector resolution, which makes it possible to measure changes in the magnetic ordering wavevector with very high accuracy. Thirdly, XRS is particularly useful for the case of DyMn_2O_5 because the neutron absorption cross section for ¹⁶⁴Dy is relatively large and this isotope makes up about 28% of naturally occurring Dy. Hence, it is difficult to obtain a good signal to background ratio in a neutron diffraction measurement on DyMn_2O_5 . The advantages of XRS have enabled us in this study to clarify the existing data on DyMn_2O_5 , and to provide a more detailed picture of the various ordering features of this important multiferroic material.

II. EXPERIMENTAL DETAILS

The single crystal sample was grown using the flux method²⁴. Preliminary x-ray measurements using a standard Laue camera showed that the lattice parameters and space group of the sample used were consistent with those expected from the literature.

Magnetometry measurements were performed using a Quantum Design SQUID magnetometer, and exhibited the same behaviour as previously reported¹⁵. Specific heat measurements were performed in zero applied magnetic field using a Quantum Design PPMS. After alignment of the crystal with the x-ray Laue the sample was cut and polished so that the $(0, 0, 1)$ direction was normal to the surface. Most of the synchrotron x-ray measurements were made at wavevectors of the form $\mathbf{Q} = (0, 0, 4) \pm \mathbf{q}$.

X-ray resonant scattering (XRS) and non-resonant x-ray scattering measurements were performed on the XMaS beamline at the European Synchrotron Radiation Facility (ESRF), Grenoble, France. The source of x-rays at XMaS is a bending magnet, so the light is linearly polarised in the horizontal plane. A vertical scattering geometry was used, shown in Figure 1, so the incoming

x-rays were σ -polarised. For the XRS measurements an incident energy of 7.795 keV, corresponding to the Dy L_3 -edge (see below), was used. For non-resonant measurements an incident energy of 11.17 keV was used. For the XRS measurements at the Dy L_3 -edge a Au(222) analyser crystal between the sample and detector was used in order to measure the σ' and π' polarised components in the scattered beam.

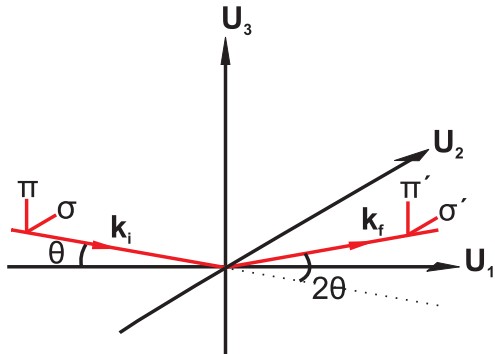


FIG. 1: (Color online) The vertical x-ray scattering geometry, defining U_1 , U_2 and U_3 , as well as the polarisation directions and scattering angle 2θ

The magnetic scattering amplitude in XRS, for each polarisation state, is given by²⁵

$$\begin{aligned} \mathbf{A}_{\text{res}}^{\text{Mag}} &= \begin{pmatrix} \sigma \rightarrow \sigma' & \sigma \rightarrow \pi' \\ \pi \rightarrow \sigma' & \pi \rightarrow \pi' \end{pmatrix} \\ &= F_{E1}^{(1)} \begin{pmatrix} 0 & z_1 \cos\theta + z_3 \sin\theta \\ z_3 \sin\theta - z_1 \cos\theta & -z_2 \sin 2\theta \end{pmatrix} \end{aligned} \quad (1)$$

where z_1 is parallel to U_1 and so on (see Figure 1).

The Dy L_3 -edge, which involves virtual electronic transitions between the $2p$ and $5d$ states, was used for XRS measurements because the resonant enhancement of the magnetic scattering at this energy can be several orders of magnitude. This contrasts with the resonant enhancement of magnetic scattering at the Mn K -edge ($1s \rightarrow 4p$), which is only a factor of about 3. Furthermore, the spectrum of the bending magnet source at XMaS is such that the flux of x-rays with energies near the Dy L_3 -edge is significantly higher than the flux of x-rays with energies near the Mn K -edge. Thus one would expect it to be possible to observe magnetic scattering arising from ordering on both the Mn and Dy sublattices by measuring the signal from the Dy sublattice alone, assuming that the magnetic polarisation of the $5d$ states of the Dy ions is caused by a combination of the local magnetic environment due to the Mn ions and the magnetisation of the Dy $4f$ electrons.

An energy of 11.17 keV was chosen for the non-resonant measurements for two reasons. First, at higher x-ray energies the penetration depth of the x-rays is larger, thus increasing the scattering volume and making the signal

less surface sensitive. This means that any observed signal is both more intense and sharper in wavevector than it would be for lower energies. Second, this energy is sufficiently high that although the flux of x-rays from the bending magnet is still very high, the flux of higher harmonic x-rays is vastly smaller. This effectively eliminates the possibility of mistaking scattering at this energy with scattering resulting from second or third harmonic x-rays.

III. RESULTS

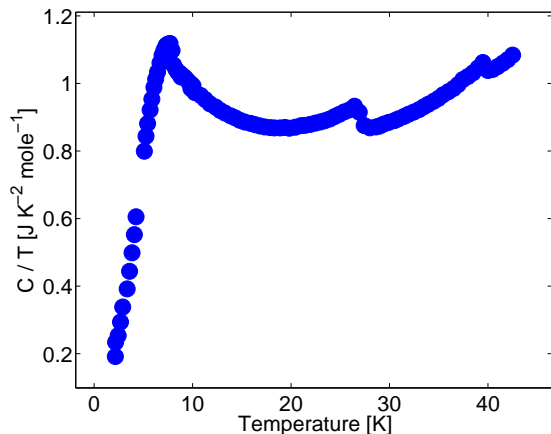


FIG. 2: (Color online) Measurement of the specific heat of the crystal of DyMn_2O_5 used in the x-ray measurements. The temperatures at which there are anomalies agree with those measured previously^{15,17}. Note that the lattice specific heat has not been subtracted from these data.

The specific heat of the sample used for this XRS study is shown in Figure 2. There are clear anomalies at $T = 7.2$ K, 27 K and 39 K, which is in agreement with previous measurements of the specific heat¹⁷.

The first XRS measurements we describe were designed to confirm the existence of antiferromagnetic (AFM) order on the Dy ions at low temperatures, an effect which is seemingly ubiquitous in the RMn_2O_5 compounds when R is magnetic. Figure 3(a) shows the integrated intensity and position in reciprocal space of the scattering arising from the Dy AFM order. On warming, the intensity of the scattering decreases monotonically, as expected, until T_N^{Dy} is reached. However, between roughly 4.5 K and 5 K the ordering wavevector of the Dy ions suddenly changes from $(0.5, 0, 0)$ to $(0.52, 0, 0)$. Such an effect has not previously been observed in neutron or x-ray scattering measurements on any of the RMn_2O_5 compounds. Figure 3(b) shows a scan of the incident x-ray energy at the $(0.5, 0, 0)$ position at 2 K. There is a clear resonance at 7.795 keV, which corresponds to virtual transitions to the $5d$ states. The resonance peak is broadened on the left-hand side by about 10 eV, and the background level on the left-hand side is higher than that on the right-hand side. Such broadening is probably due to interference between

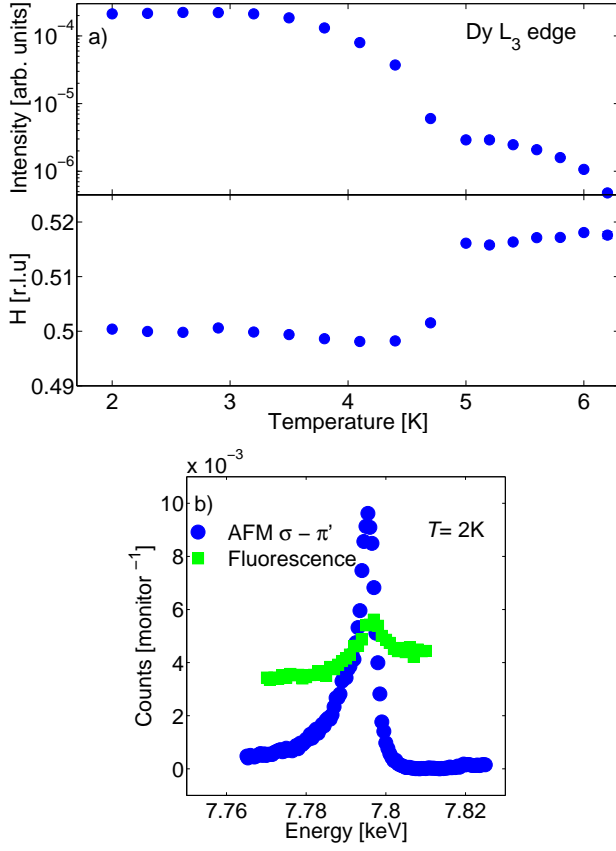


FIG. 3: (Color online) XRS from the AFM ordering of the Dy ions in DyMn_2O_5 with wavevector $\mathbf{q}_{AFM}^{Dy} = (0.5, 0, 0)$. (a) Results of fits to the peak in scans parallel to $(H, 0, 0)$ to a Gaussian lineshape. Notice that the intensity is plotted on a logarithmic scale, and that the incommensurate signal is two orders of magnitude weaker than the AFM signal. Above 6.2K the intensity became so weak as to be below the detection threshold of the apparatus. (b) Scans of the incident x-ray energy at fixed wavevector $\mathbf{q}_{AFM}^{Dy} = (0.5, 0, 0)$, showing a strong resonance at the Dy L_3 edge (blue triangles) and the sample fluorescence (green squares, rescaled).

resonant and non-resonant magnetic scattering^{26,27}. Figure 3(b) also shows the sample fluorescence, which has been rescaled because a different detector was used to measure it.

Figure 4 shows the temperature dependence of the intensity and wavevector of the magnetic signal associated with the order on the Mn sublattice. The scattering was measured at several ICM wavevectors of the form $\mathbf{Q} = (0, 0, 4) + \mathbf{q}_{ICM}$ where $\mathbf{q}_{ICM} = (\pm 0.5 \pm \delta, 0, \pm 0.25 \pm \epsilon)$. At low temperatures this ICM phase has non-zero δ and ϵ . Between $T = 2\text{ K}$ and $T = 19\text{ K}$ δ increases slightly from about -0.023 to -0.018 , and ϵ increases almost linearly from -0.015 to zero, then changes sign and increases further to 0.007 . The intensity of the scattering has a maximum at 5 K, the same temperature at which the Dy AFM order disappears. Above 5 K the intensity decreases steadily, and eventually falls below the detec-

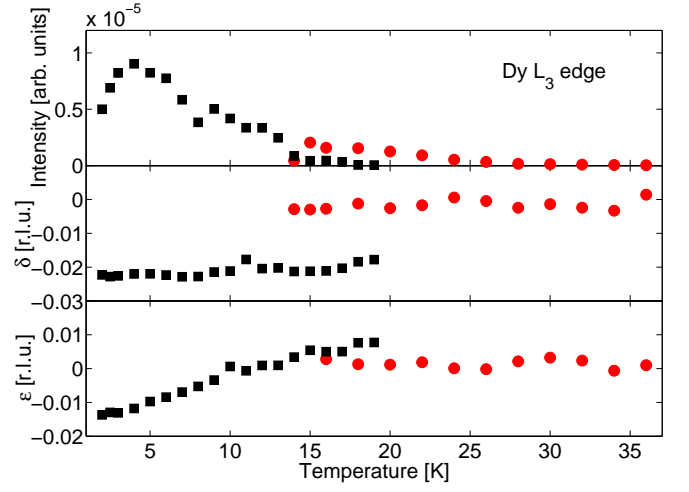


FIG. 4: (Color online) XRS data from DyMn_2O_5 at the wavevectors $\mathbf{q}_{ICM} = (-0.5 + \delta, 0, 0.25 + \epsilon)$ (filled squares) and $\mathbf{q}_{CM} = (-0.5, 0, 0.25)$ (filled circles). Diffraction peaks were fitted to a Gaussian lineshape for scans parallel to $(H, 0, 0)$, and to a Lorentzian-squared for scans parallel to $(0, 0, L)$. The integrated intensity shown in the top panel is the product of the Gaussian amplitude and width at each temperature. The error bars are smaller than the size of the points.

tion threshold at $T = 19\text{ K}$.

Figure 4 also shows that for $T \geq 14\text{ K}$ a CM phase appears, i.e. one for which $\mathbf{q}_{CM} = (0.5, 0, 0.25)$. The intensity of this signal grows upon warming, becoming stronger than the ICM signal by 15 K, where it also reaches a maximum. The maximum intensity of the CM signal is a factor of 5 weaker than the maximum intensity of the ICM signal. As temperature is increased above 15 K the intensity of the scattering gradually decreases, falling below the detection threshold for $T > 37\text{ K}$.

Signals were measured at the equivalent positions $\mathbf{q}_1 = (-0.5 + \delta, 0, 0.25 - \epsilon)$, $\mathbf{q}_2 = (-0.5 - \delta, 0, 0.25 - \epsilon)$ and $\mathbf{q}_3 = (-0.5 + \delta, 0, -0.25 + \epsilon)$ for several temperatures. Although the same behaviour was observed at each position the absolute intensity of the signal was strongest at \mathbf{q}_2 , probably due to a certain amount of self-absorption of x-rays by the crystal in the other orientations. The intensity and wavevector at each temperature were determined by fitting the lineshape in scans parallel to $(H, 0, 0)$ to a Gaussian, and scans parallel to $(0, 0, L)$ to a Lorentzian-squared function. These functions were chosen because they gave the best fit to the data. The maximum intensities of these signals were at least an order of magnitude smaller than the signal arising from the AFM order of the Dy ions. To illustrate this, Figure 5 displays the intensities of each type of magnetic peak as a function of temperature, on a logarithmic scale.

Figure 6 shows scans of the incident x-ray energy through the Dy L_3 -edge at the ICM wavevector $(0.5 + \delta, 0, 0.25 + \epsilon)$. The strong resonance shows that the signal observed in this experiment is due to the magnetic interaction ‘felt’ by the electrons excited into the $5d$ states

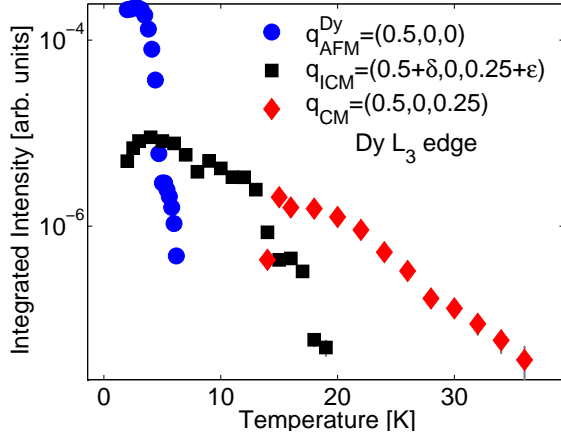


FIG. 5: (Color online) Integrated intensity of the Dy-AFM, ICM and CM signals, plotted on a logarithmic scale. The coupling between Dy and Mn ions in the ICM and CM phases, given by the order of magnitude of the intensity, appears to decrease approximately as a power law with increasing temperature.

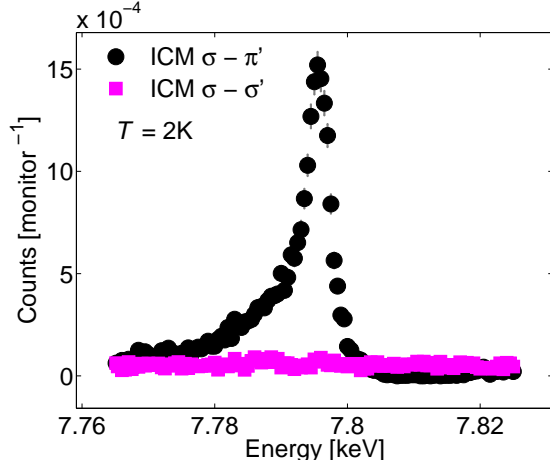


FIG. 6: (Color online) Scans of the incident x-ray energy for the ICM signal at $(0.5 + \delta, 0, 0.25 + \epsilon)$. The strong peaks in the $\sigma - \pi'$ channel, together with a lack of signal in the $\sigma - \sigma'$ channel, shows that the scattering is purely magnetic at this wavevector.

caused by the magnetic order of the surrounding Mn ions. The scattering is entirely in the $\sigma - \pi'$ polarisation channel, with nothing in the $\sigma - \sigma'$ channel, which shows that this ordering is magnetic and essentially dipolar, since any quadrupolar term, which would appear in the $\sigma - \sigma'$ channel, is immeasurably small. The broadening of the resonance peak at energies below the Dy L_3 edge presumably has the same origin as that discussed earlier in relation to Figure 3(b), i.e. interference between non-resonant magnetic scattering and resonant magnetic scattering.

Figure 7 shows how the widths of the AFM, ICM and CM peaks vary with temperature for scans parallel to

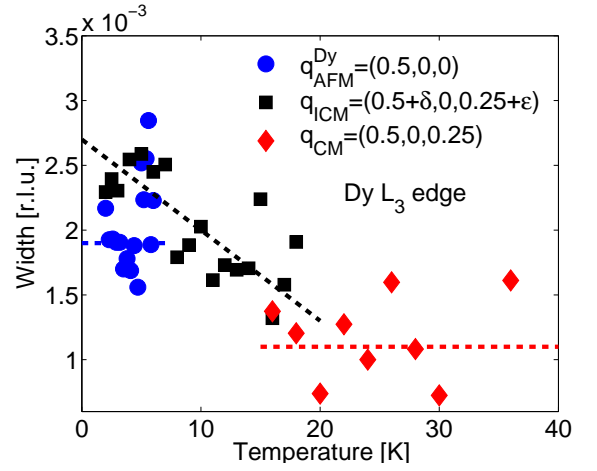


FIG. 7: (Color online) The widths (FWHM) of the peaks corresponding to the Dy AFM, ICM and CM order measured in scans parallel to $(0, 0, L)$. The widths were determined by moment analysis. The dashed lines are guides to the eye. Similar analysis of scans parallel to $(H, 0, 0)$ and $(0, K, 0)$ (not shown) shows no change in the width in these directions.

$(0, 0, L)$. The peaks are fitted to a Lorentzian-squared lineshape. It is clear that the correlation length, proportional to $1/(\text{width})$, is shorter for the ICM order at low temperatures than for the Dy AFM and the CM order at higher temperatures. Indeed, the correlation length of the order on the electrons spins in the $5d$ states of the Dy ions, induced by the Mn sublattice ordering, increases with increasing temperature, before becoming constant above about 20 K.

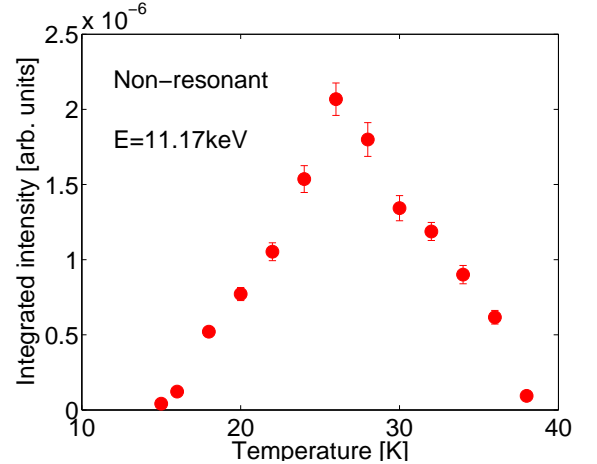


FIG. 8: (Color online) Temperature variation of the intensity of the signal at $\mathbf{q} = (0, 0, 0.5)$ measured with a non-resonant x-ray energy. The intensities were calculated from fits to a Gaussian for scans parallel to $(H, 0, 0)$. This scattering is due to a change in the crystal structure.

Figure 8 shows the results of non-resonant x-ray scattering measurements made with an incident x-ray energy of 11.17 keV, plotting the intensity of the signal

at $\mathbf{Q} = (0, 0, 4.5) = (0, 0, 4) + 2\mathbf{q}_{CM}$, versus temperature. At no temperature was a signal corresponding to $(0, 0, 4) \pm 2\mathbf{q}_{ICM}$ observed. The signal at $2\mathbf{q}_{CM}$ appears at $T = 15$ K and its intensity increases steadily with warming, reaching a maximum at 27 K. On further warming the intensity decreases until it becomes too weak to measure at $T > 38$ K. This measurement is in complete agreement with the x-ray scattering data of Higashiyama *et al.*¹⁷ on the same material. Interestingly, the temperature at which this signal is a maximum is the same temperature at which there is a distinct anomaly in the specific heat (see Figure 2), and at which the FE polarisation reaches a local maximum¹⁷. Since this peak occurs in a non-magnetic, non-resonant channel it must arise from Thompson scattering, i.e. scattering of the x-rays by the charge of the ions in the system, and therefore be structural in origin.

IV. DISCUSSION

XRS methods have been used to examine the magnetic ordering in DyMn_2O_5 by measuring the magnetism on the Dy ions induced by the magnetic environment of the surrounding Mn ions. Several observations have been made which go beyond previous neutron scattering studies of this compound. Specifically these are:

1. The existence of a structural distortion, characterised by $\mathbf{q} = (0, 0, 0.5)$, for $15 \text{ K} \leq T < 40 \text{ K}$, coexistent with the strongest FE polarisation.
2. The existence of magnetic interactions in the $5d$ states of the Dy ions induced by the magnetism of the surrounding Mn sublattice. This is an effect which is present for $T \leq T_N \approx 40 \text{ K}$, and not just below 8 K ($T \leq T_N^{Dy}$).
3. Changes in the H component of the wavevector of the ICM order for $2 \text{ K} \leq T \leq 19 \text{ K}$, and indeed non-zero incommensurability of this H component, as well as an incommensurate L component.

There have also been observed differences with XRS measurements on the related compound TbMn_2O_5 :

1. No sign of a re-entrant ICM phase at higher temperatures.
2. The existence of an ICM phase with negative ϵ as well as positive ϵ , as opposed to the phase with only positive ϵ observed by Okamoto *et al.*²².

In addition, this study goes beyond all previous scattering studies by measuring changes in the widths of the various peaks with temperature. Finally, the existence of a previously undetected magnetic ordering wavevector of $\mathbf{q} = (0.52, 0, 0)$ between 5 K and T_N^{Dy} was observed.

There are, of course, many similarities between the findings in this study and the findings of previous studies

which used neutron scattering to examine DyMn_2O_5 , or XRS to measure TbMn_2O_5 :

1. The existence of two distinct phases below T_N , namely the ICM and CM phases.
2. Changes in the incommensurability of the ICM signal with changing temperature.
3. The existence of antiferromagnetic order on the Dy ions at low temperatures.

The change in wavevector of the AFM order from $(0.5, 0, 0)$ to $(0.52, 0, 0)$ shown in Figure 3, which has not been observed in neutron scattering measurements or indeed in XRS measurements of other RMn_2O_5 compounds, might be explained as follows. The Dy $4f$ spins are coupled antiferromagnetically, and so the exchange Hamiltonian contains terms which are proportional to μ_{Dy}^2 , the square of the ordered Dy magnetic moments. With increasing temperature the ordered moment reduces, causing the exchange energy to decrease rapidly. There is also an exchange interaction between the ordered $4f$ spins and the $5d$ states, and this too weakens in the same way. Coexistent with the Dy–Dy interaction there also exists a coupling between the Dy $5d$ spin states and the Mn spins. The Mn spins order at a much higher temperature and therefore their average magnetic moment remains fairly constant at the low temperatures under consideration. This means the exchange energy of the Dy–Mn coupled system will reduce much less. At low temperatures the Dy–Dy interaction dominates over the Dy–Mn coupling, but as temperature increases the two couplings eventually become similar in strength. This may allow the H -component of the Dy $5d$ magnetic order to become entrained to the ICM order of the Mn sublattice. Further support for such an interpretation is found from the widths of the peaks in scans parallel to $(0, 0, L)$ shown in Figure 7. The change of wavevector from $(0.5, 0, 0)$ to $(0.52, 0, 0)$ is accompanied by a sudden increase in the width to a value similar to that of the ICM phase. If indeed the competition between Dy–Dy AFM coupling and Dy–Mn ICM coupling causes the change in wavevector then one might expect the width of the peak at $(0.52, 0, 0)$ to be similar to that of the ICM peak at the same temperature.

To reiterate, the data presented show that the Dy $5d$ bands show some magnetic order right up to the Néel temperature of the Mn sublattice. Since the measurements presented in this paper show only the magnetic order on the Dy $5d$ states there are two possible ways to account for the changes in the width of the L -component of the ICM and CM peaks, shown in figure 7. The first is that there is some magnetisation of the Dy $4f$ electrons, which polarises the $5d$ states, and there is some change in the correlation length of this. The second is that there is a change in the magnetic order of the Mn which is then reflected as a change in the Dy magnetic order. In the first case it is possible that the correlation length of the

magnetically ordered Dy sublattice itself changes with temperature, with the Mn correlation length remaining fixed, i.e. the Dy magnetic correlation length does not reflect the Mn magnetic correlation length. In the second case it is possible that the Dy $5d$ and Mn magnetic correlation lengths behave in the same way as a function of temperature, and it is the Mn correlation length that changes. In either case the correlation length appears only to change along the c -axis, and not along the a - or b -axes, evidenced by the change in the width of the L-components but not in the H- or K-components of the peaks (not shown).

One possible explanation of the increased L width in the ICM phase compared to the CM phase is that the magnetic structure is broken up into locally commensurate domains between which there exist ‘slips’ which have the overall effect of making the magnetic structure incommensurate. Koo *et al.*²³ suggest that in TbMn_2O_5 the ICM phase may be interpreted as CM spin modulations with domain walls, analogous to an effect observed in $\text{ErNi}_2\text{B}_2\text{C}$ ²⁸. The measurements detailed above would appear to support such an interpretation, with domain walls in the ab -plane.

The non-resonant scattering measured at $2\mathbf{q}_{CM} = (0, 0, 0.5)$, which is structural in origin, ties in with a model proposed to explain multiferroicity in TbMn_2O_5 ²⁹ and later extended to describe YMn_2O_5 ³⁰. The RMn_2O_5 materials are geometrically frustrated, with five different exchange interactions identified between the Mn ions, and it is clear that one way to lift the resulting degeneracy would be a small structural distortion. Analysis of the atomic displacement parameters²⁹ suggests that a canted antiferroelectric (CAF) structural phase may be the way in which this degeneracy is lifted. In this case the lattice distorts in the opposite sense in adjacent unit cells along the c -axis, but in the same sense along the a - and b -axes. In each unit cell the distortions along the a -axis of different ions are in different directions such that the FE polarisation along the a -axis is cancelled out, however this does not occur for the distortions along the b -axis. This would then give rise to a FE polarisation along the b -axis, which is indeed what is observed. A difficulty with this explanation of the occurrence of ferroelectricity in DyMn_2O_5 , however, is that the amplitude of the scattering at $2\mathbf{q}_{CM}$ does not map on to the amplitude of the observed FE polarisation. The polarisation does have a local maximum at the same temperature at which the scattering at $2\mathbf{q}_{CM}$ is most intense, $T_{max} = 27\text{K}$, but the onset of the largest polarisation is actually at about 17K, and the signal at $2\mathbf{q}_{CM}$ is relatively weak at this temperature.

Several phenomenological theories have been proposed to explain the occurrence of multiferroicity^{11,12,13,31}. A successful approach for the RMnO_3 compounds has been developed by Mostovoy¹² which uses symmetry considerations combined with a direct magnetoelectric coupling. The theory shows that certain types of spiral magnetic order can induce a FE polarisation. Such an approach

has proved very successful at explaining the multiferroic behaviour of TbMnO_3 , in particular. A modified version of this approach has been suggested by Betouras *et al.*¹³ to account for the multiferroic properties of the RMn_2O_5 -type compounds, in which the same starting point of considering the free energy in a Landau model is used, but with additional assumptions. These assumptions are that the spin density wave (SDW) that couples to the FE polarisation is *acentric*, i.e. the spin density is not necessarily centred on a lattice site and has a non-zero phase, and that the polarisation and inverse ferroelectric susceptibility have small oscillatory parts in addition to a constant term. The result of this is that a spontaneous polarisation is only allowed for magnetic phases which are *commensurate*. It is clear that in DyMn_2O_5 the polarisation is much larger in the CM phase, so the present data tend to support this explanation.

As mentioned in the introduction, the magnitude of the FE polarisation in DyMn_2O_5 is the strongest of all the materials in the RMn_2O_5 family. The results presented in this paper show that there is a significant magnetic interaction in the Dy $5d$ bands, and it is possible that there is also an induced ordering of the partially occupied Dy $4f$ states. It has been found previously that the size of the ordered moment of the Dy ions in DyMn_2O_5 is larger than that of other rare earth ions in the RMn_2O_5 series¹⁹, which might partly explain why such a clear signal at the Dy L-edge resonance is observed here. The models used to explain multiferroic effects discussed above do not constrain the magneto-electric coupling to involve just the Mn ions, so in principle magnetic order of the Dy ions with the same wavevector as the magnetic order of the Mn ions could give rise to an ‘extra’ contribution to the FE polarisation through the same mechanism. If such coupling were proportional to the size of the rare-earth moment then that might explain the existence of the strongest polarisation in DyMn_2O_5 and the weakest polarisation in YMn_2O_5 among the RMn_2O_5 materials.

V. CONCLUSIONS

In conclusion, the XRS measurements presented here have shown that the magnetic ordering in DyMn_2O_5 bears many similarities to that of other members of the RMn_2O_5 family of materials previously studied. These measurements also show extra features not previously observed in neutron scattering measurements on DyMn_2O_5 . Of particular note is the observation that the Dy $5d$ bands are magnetically polarised right up to $T_N \sim 40\text{K}$, the Néel temperature of the Mn ions. If the $4f$ states are magnetised in a similar fashion there may be an enhancement of the ferroelectric polarisation in this material, given the large Dy magnetic moment. Such measurements demonstrate that x-ray resonant scattering is a powerful tool for studying materials in which there exists more than one magnetic ion, in particular allowing one to resonantly enhance the scattering from magnetic

order on one sublattice which has been induced by the magnetisation of the other sublattice.

VI. ACKNOWLEDGEMENTS

We thank F.R. Wondre for x-ray Laue alignment of the sample, P.J. Baker for assistance with the heat ca-

capacity measurements, and S.J. Blundell for useful discussions. We are grateful for financial support from the Engineering and Physical Sciences Research Council of Great Britain and from the Wolfson Royal Society Research Merit Award scheme (DFM).

-
- * Electronic address: r.ewings1@physics.ox.ac.uk
- ¹ E.F. Bertaut and M. Mercier, *Mat. Res. Bull.* **6**, 907 (1971)
 - ² I.E. Dzyaloshinskii, *Sov. Phys. JETP* **10**, 628 (1960)
 - ³ D.N. Astrov, *Sov. Phys. JETP* **11**, 708 (1960)
 - ⁴ G.T. Rado and V.J. Folan, *Phys. Rev. Lett.* **7**, 310 (1961)
 - ⁵ B.I. Al'shin and D.N. Astrov, *Sov. Phys. JETP* **17**, 809 (1963)
 - ⁶ G.T. Rado, *Phys. Rev. Lett.* **13**, 335 (1964)
 - ⁷ E. Fischer, G. Gorodetsky, and R.M. Hornreich, *Solid State Commun.* **10**, 1127 (1972)
 - ⁸ L.M. Holmes, L.G. van Uitert, and G.W. Hull, *Solid State Commun.* **9**, 1373 (1971)
 - ⁹ T. Kimura, T. Goto, H. Shintani, K. Ishizaka, T. Arima, and Y. Tokura, *Nature (London)* **426**, 55 (2003)
 - ¹⁰ T. Goto, T. Kimura, G. Lawes, A.P. Ramirez, and Y. Tokura, *Phys. Rev. Lett.* **92**, 257201 (2004)
 - ¹¹ M. Kenzelmann, A.B. Harris, S. Jonas, C. Broholm, J. Schefer, S. B. Kim, C. L. Zhang, S.-W. Cheong, O. P. Vajk, and J. W. Lynn, *Phys. Rev. Lett.* **95**, 087206 (2005)
 - ¹² M. Mostovoy, *Phys. Rev. Lett.* **96**, 067601 (2006)
 - ¹³ J.J. Betouras, G. Giovannetti, and J. van den Brink, *Phys. Rev. Lett.* **98**, 257602 (2007)
 - ¹⁴ N. Hur, S. Park, P.A. Sharma, J. S. Ahn, S. Guha, and S.-W. Cheong, *Nature (London)* **429**, 392 (2004)
 - ¹⁵ N. Hur, S. Park, P.A. Sharma, S. Guha, and S.-W. Cheong, *Phys. Rev. Lett.* **93**, 107207 (2004)
 - ¹⁶ D. Higashiyama, S. Miyasaka, and Y. Tokura, *Phys. Rev. B* **72**, 064421 (2005)
 - ¹⁷ D. Higashiyama, S. Miyasaka, N. Kida, T. Arima, and Y. Tokura, *Phys. Rev. B* **70**, 174405 (2004)
 - ¹⁸ A. Inomata and K. Kohn, *J. Phys. Condensed Matter* **8**, 2673 (1996)
 - ¹⁹ G.R. Blake, L.C. Chapon, P.G. Radaelli, S. Park, N. Hur, S.-W. Cheong, and J. Rodríguez-Carvajal, *Phys. Rev. B* **71**, 214402 (2005)
 - ²⁰ C. Wilkinson, F. Sinclair, P. Bardner, J.B. Forsyth, and B.M.R. Wanklyn, *J. Phys. C* **14**, 1671 (1981)
 - ²¹ W. Ratcliff III, V. Kiryukhin, M. Kenzelman, S.-H Lee, R. Erwin, J. Schefer, N. Hur, S. Park, and S.-W. Cheong, *Phys. Rev. B* **72**, 060407 (2005)
 - ²² J. Okamoto, D. J. Huang, C.-Y. Mou, K.S. Chao, H.-J. Lin, S. Park, S.-W. Cheong, and C.T. Chen, *Phys. Rev. Lett.* **98**, 157202 (2007)
 - ²³ J. Koo, C. Song, S. Ji, J.-S. Lee, J. Park, T.-H. Jang, C.-H. Yang, J.-H. Park, Y.H. Jeong, K.-B. Lee, T.Y. Koo, Y.J. Park, J.-Y. Kim, D. Wermeille, A.I. Goldman, G. Srajer, S. Park, and S.-W. Cheong, *Phys. Rev. Lett.* **99**, 197601 (2007)
 - ²⁴ B.M.R. Wanklyn, *J. Mater. Sci.* **7**, 813 (1972)
 - ²⁵ J.P. Hill and D.F. McMorrow, *Acta. Cryst. A* **52**, 236 (1996)
 - ²⁶ J.P. Hill, C.-C. Kao, and D.F. McMorrow, *Phys. Rev. B* **55**, 8662 (1997).
 - ²⁷ W. Neubeck, C. Vettier, K.-B. Lee, and F. de Bergevin, *Phys. Rev. B* **60**, 9912 (1999).
 - ²⁸ H. Kawano-Furukawa, H. Takeshita, M. Ochiai, T. Nagata, H. Yoshizawa, N. Furukawa, H. Takeya, and K. Kadowaki, *Phys. Rev. B* **65**, 180508 (2002)
 - ²⁹ L.C. Chapon, G.R. Blake, M.J. Gutmann, S. Park, N. Hur, P.G. Radaelli, and S.-W. Cheong, *Phys. Rev. Lett.* **93**, 177402 (2004)
 - ³⁰ L.C. Chapon, P.G. Radaelli, G.R. Blake, S. Park, and S.-W. Cheong, *Phys. Rev. Lett.* **96**, 097601 (2006)
 - ³¹ H. Katsura, N. Nagaosa, and A.V. Balatsky, *Phys. Rev. Lett.* **95**, 057205 (2005)